Spectral distortion of dual-comb spectrometry due to repetition rate fluctuation*

Hong-Lei Yang(杨宏雷), Hao-Yun Wei(尉昊赟), and Yan Li(李岩)†

State Key Laboratory of Precision Measurement Technology & Instruments, Department of Precision Instrument, Tsinghua University, Beijing 100084, *China*

(Received 12 October 2015; revised manuscript received 15 November 2015; published online 20 February 2016)

Dual-comb spectrometry suffers the fluctuations of parameters in combs. We demonstrate that the repetition rate is more important than any other parameter, since the fluctuation of the repetition rate leads to a change of difference in the repetition rate between both combs, consequently causing the conversion factor variation and spectral frequency misalignment. The measured frequency noise power spectral density of the repetition rate exhibits an integrated residual frequency modulation of 1.4 Hz from 1 Hz to 100 kHz in our system. This value corresponds to the absorption peak fluctuation within a root mean square value of 0.19 cm^{-1} that is verified by both simulation and experimental result. Further, we can also simulate spectrum degradation as the fluctuation varies. After modifying misaligned spectra and averaging, the measured result agrees well with the simulated spectrum based on the GEISA database.

Keywords: optical frequency comb, Infrared spectra, molecular spectra

PACS: 42.62.Eh, 33.20.Ea, 33.20.–t **DOI:** 10.1088/1674-1056/25/4/044207

1. Introduction

An optical frequency comb,[1] providing hundreds of thousands of even spaced and mutual coherent longitudinal modes which are traced to frequency standard, pushes laser metrology forward by a tremendous step including molecular spectroscopy.[2] Based on multi-heterodyne detection that is similar to conventional Fourier transform spectrometry,[3] a dual-comb spectrometer employs two comb lasers with slightly different repetition rates to mimic scanning sampling. In this scenario, detuned pulse trains act as asynchronous optical sampling probes for each other.[4,5] Thus, a dual-comb system can also be applied to monitor instantaneous phenomenon[6] or remote, fast sensing.[7] Because of the unique measurement principle, it has many advantages, such as high-speed acquisition, high resolution, and high-frequency accuracy.

To a remarkable extent, the three 'High' advantages are confined by comb laser performance. In one comb, there are two freedoms, i.e., repetition rate ($f_{\rm rep}$) and carrier-envelope offset frequency ($f_{\rm ceo}$). The stabilities of $f_{\rm rep}$ and $f_{\rm ceo}$ directly affect the performance of the measurement system. In order to record non-distorted interferograms by a dual-comb spectrometer, one method is to use highly stabilized laser combs via phase-locking both freedoms to optical frequency standards.[8,9] Owing to the precise control of laser combs, the radio frequency (RF) beats generated by pairs of nearby comb modes are fixed. Alternatively, a raw distorted interferogram of free-running laser combs can be corrected by mixing adaptive signals which contain phase error information on real-time compensation hardware[10] or by a posteriori correction algorithm.[11,12] No frequency standards in these systems cause a little trouble in mapping spectral features along the horizontal axis. However, these studies show the solution of laser fluctuation, but they do not include how the spectrum degrades since laser performance deteriorates.

In this paper, the frequency stabilities of $f_{\rm rep}$ and $f_{\rm ceo}$ are evaluated. According to the principle, the repetition rate fluctuation is the main reason that causes spectral frequency misalignment compared with carrier-envelope offset frequency variation. By establishing a dual-comb system traced to a Rubidium clock, we measure the P branch in the $2\nu_3$ rotational–vibrational band of hydrogen cyanide ($H^{13}C^{14}N$). The measured spectra show absorption peak jitter that is in agreement with unstable pulse interference simulation. The signal-to-noise ratio of the absorption spectrum is effectively improved by averaging modified spectra in the frequency domain. Finally, discussion and further improvement are presented.

2. Measurement principle and frequency fluctuation

A well-stabilized mode-locked laser provides a train of ultrafast pulses at a constant repetition rate and with equal carrier-envelope phase shift in the time domain. In the optical domain, the comb structure of laser modes extends hundreds of nanometers in the optical domain. The output field can be

*Project supported by the State Key Laboratory of Precision Measurement Technology & Instruments of Tsinghua University and the Young Scientists Fund of the National Natural Science Foundation of China (Grant No. 61205147).

†Corresponding author. E-mail: liyan@mail.tsinghua.edu.cn

© 2016 Chinese Physical Society and IOP Publishing Ltd

described as

$$E_1(t) = \sum_{n=1}^{\infty} A_{1,n} \exp\left[-\mathrm{i}2\pi\left(n \cdot f_{\mathrm{rep}} + f_{\mathrm{ceo}}\right)t\right], \quad (1)$$

where A is the amplitude of the longitudinal mode and n is the mode number. If a gas cell is inserted into the path, this beam will be attenuated and phase shifted since some components resonate with rotational-vibrational energy levels of gas under test. Equation (1) should be modified into

$$\begin{aligned} E_1(t) &= \sum_{n=1}^{\infty} A_{1,n} \exp\left(-\alpha_{1,n} - \mathrm{i}\varphi_{1,n}\right) \\ &\quad \times \exp\left[-\mathrm{i}2\pi\left(n \cdot f_{\mathrm{rep}} + f_{\mathrm{ceo}}\right)t\right], \end{aligned} \quad (2)$$

where α is the amplitude attenuation coefficient of the electric field and φ is the phase shift induced by the gas sample. Similarly, the secondary laser comb is expressed as

$$\begin{aligned} E_2(t) &= \sum_{n=1}^{\infty} A_{2,n} \exp\left(-\alpha_{2,n} - \mathrm{i}\varphi_{2,n}\right) \\ &\quad \times \exp\left\{-\mathrm{i}2\pi\left[n \cdot \left(f_{\mathrm{rep}} + \Delta f_{\mathrm{rep}}\right)\right.\right. \\ &\quad \left.\left. + \left(f_{\mathrm{ceo}} + \Delta f_{\mathrm{ceo}}\right)\right]t\right\}, \end{aligned} \quad (3)$$

where Δf_{rep} is the difference between the repetition rates and Δf_{ceo} is the difference between both carrier-envelope offset frequencies. Then the superposition field is obtained by a square-law photodiode as

$$\begin{aligned} I(t) &\propto \left|E_1(t) + E_2(t)\right|^2 \propto \mathrm{Re}[E_1^*(t)E_2(t)] \\ &\propto \mathrm{Re}\left\{\sum_{n,m} A_{1,m}^* A_{2,n} \exp\left(-\alpha_{1,m} - \alpha_{2,n} + \mathrm{i}\varphi_{1,m} - \mathrm{i}\varphi_{2,n}\right)\right. \\ &\quad \left.\times \exp\left\{-\mathrm{i}2\pi\left[n \cdot \Delta f_{\mathrm{rep}} + \Delta f_{\mathrm{ceo}} + (m-n) f_{\mathrm{rep}}\right]t\right\}\right\}. \end{aligned} \quad (4)$$

To avoid aliasing, any components whose frequencies are greater than half of f_{rep} are filtered. In this case, n is equal to m. So equation (4) is simplified into

$$\begin{aligned} I(t) &\propto \mathrm{Re}\left\{\sum A_{1,n} A_{2,n}^* \exp\left(-2\alpha_{1,n}\right)\right. \\ &\quad \left.\times \exp\left[\mathrm{i}2\pi\left(n \cdot \Delta f_{\mathrm{rep}} + \Delta f_{\mathrm{ceo}}\right)\right]t\right\}. \end{aligned} \quad (5)$$

By Fourier transformation $f(\omega) = \int f(t) \cdot \exp(-\mathrm{i}\omega t)\mathrm{d}t$, the interferometric signal can be analyzed in the frequency domain as follows:

$$I(f) \propto \sum A_{1,n} A_{2,n}^* \exp\left(-2\alpha_{1,n}\right) \cdot \delta\left(f - n \cdot \Delta f_{\mathrm{rep}} - \Delta f_{\mathrm{ceo}}\right). \quad (6)$$

Equation (6) shows that different pairs of optical longitudinal modes generate a down-converting RF beat comb which perfectly reveals amplitude attenuation $\alpha(\nu)$ in the optical region. Simultaneous, parallel detection can be achieved. Continuous and periodical pulses result in a repeated interferometric signal. From Eqs. (2) and (5), the optical frequency and RF frequency are

$$f_{\mathrm{opt}} = n \cdot f_{\mathrm{rep}} + f_{\mathrm{ceo}}, \quad (7)$$

$$f_{\mathrm{RF}} = n \cdot \Delta f_{\mathrm{rep}} + \Delta f_{\mathrm{ceo}}. \quad (8)$$

By combining Eqs. (7) and (8), the relationship between RF and the optical spectrum is established as

$$\begin{aligned} f_{\mathrm{opt}} &= \left(f_{\mathrm{RF}} - \Delta f_{\mathrm{ceo}}\right) \cdot \frac{f_{\mathrm{rep}}}{\Delta f_{\mathrm{rep}}} + f_{\mathrm{ceo}} \\ &= \left(f_{\mathrm{RF}} - \Delta f_{\mathrm{ceo}}\right) \cdot \beta + f_{\mathrm{ceo}}, \end{aligned} \quad (9)$$

where β is the conversion factor that equals $f_{\mathrm{rep}}/\Delta f_{\mathrm{rep}}$. In the other configuration, i.e., only one beam interrogates the gas sample; the dispersion spectrum $\varphi(\nu)$ is a byproduct.

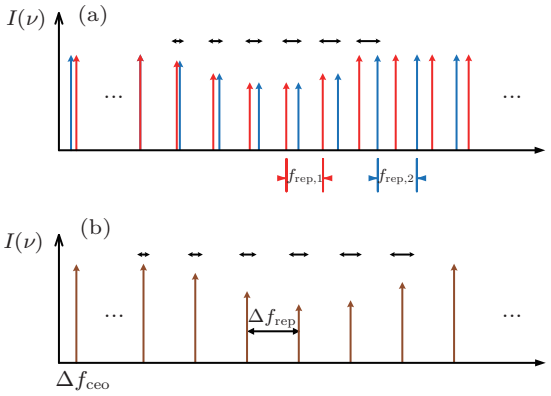


Fig. 1. (color online) Principle of dual-comb spectrometry. A two-frequency comb generates an RF beat comb according to multi-heterodyne detection. The double-sided arrow denotes laser mode fluctuation. As n goes up, the fluctuation becomes more and more considerable. (a) Optical domain, (b) RF domain.

Equation (9) demonstrates that the absorption peak fluctuation, including the zooming and shifting effect originating from f_{rep} and f_{ceo} variation, would happen if laser modes could not keep fixed during measurement. Between these two unstable parameters, the former is more critical than the latter, because a small offset in Δf_{rep} makes a large change in β, further resulting in spectral frequency misalignment. What is more, since the stabilization strategy of f_{rep} directly locks to the RF frequency standard, the phase noise of the comb mode in the optical region is n^2 times larger than that of f_{rep}. Considerable phase noise of the mode in the optical region reduces the signal-to-noise ratio of the interferometric signal. Given this, some methods mentioned in the previous section come into use.

3. Experimental setup and result

The schematic of the experimental setup is illustrated in Fig. 2. Two Er-doped fiber optical frequency combs (M-Comb, Menlo Systems) locked at $f_{\mathrm{rep}} \sim 250$ MHz provide pulse trains with an average power of ~ 20 mW and a duration of ~ 80 fs. The 20-dB output bandwidths stretch for 100 nm around 1.55 μm just as indicted in the inset in Fig. 2. The carrier-envelope offset frequencies are self-referenced with f–$2f$ interferometers.[13] All phase lock loops are referred to as

an Rb clock (Symmetricom, 8040C). With the help of quarter wave plates, half wave plates and polarized beam splitters, the polarization and power of each beam are fine-adjusted to improve modulation depth and avoid detector saturation. A region of interest, i.e., the $2\nu_3$-P rotational–vibrational band of $H^{13}C^{14}N$, is selected by an optical band-pass filter (Thorlabs, FB1550-12). The combined beam, outgoing from a 200 Torr (1 Torr = 1.33322×10^2 Pa), 7cm-long $H^{13}C^{14}N$ gas cell, is aligned to an InGaAs photodetector with a bandwidth of 125 MHz (New Focus, 1811-FS). A high-speed data acquisition system based on a field programmable gate array (National Instruments) is synchronized to one of the laser combs.

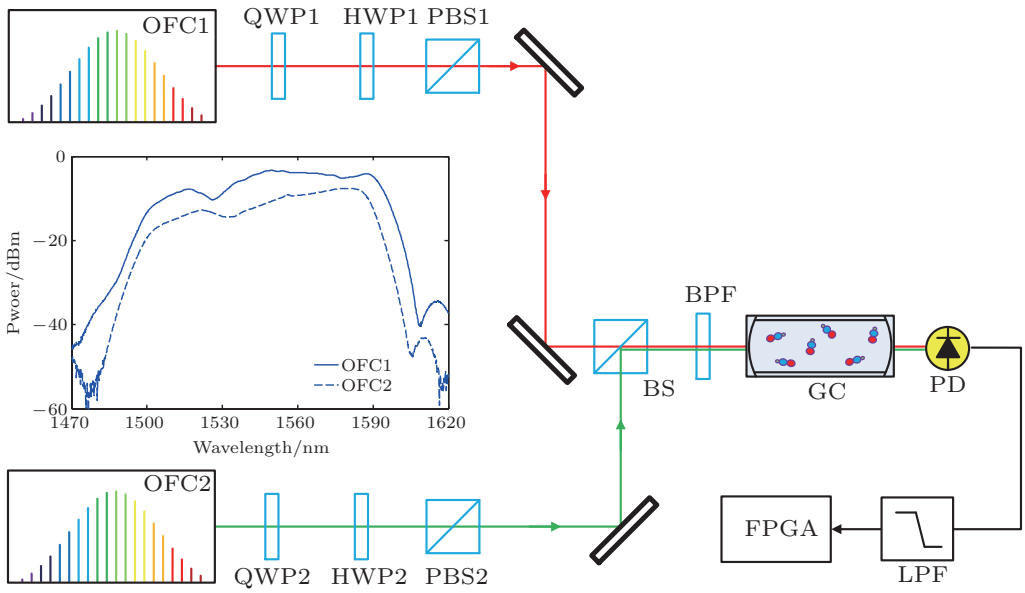


Fig. 2. (color online) Dual-comb spectrometer. The inset shows the output spectra of the frequency combs. Colorful lines represent optical beams, while black lines are electric cables. OFC: optical frequency comb; QWP: quarter waveplate; HWP: half waveplate; PBS: polarized beam splitter; BS: non-polarized beam splitter; BPF: optical band-pass filter; GC: gas cell; PD: photodetector; LPF: electronic low-pass filter.

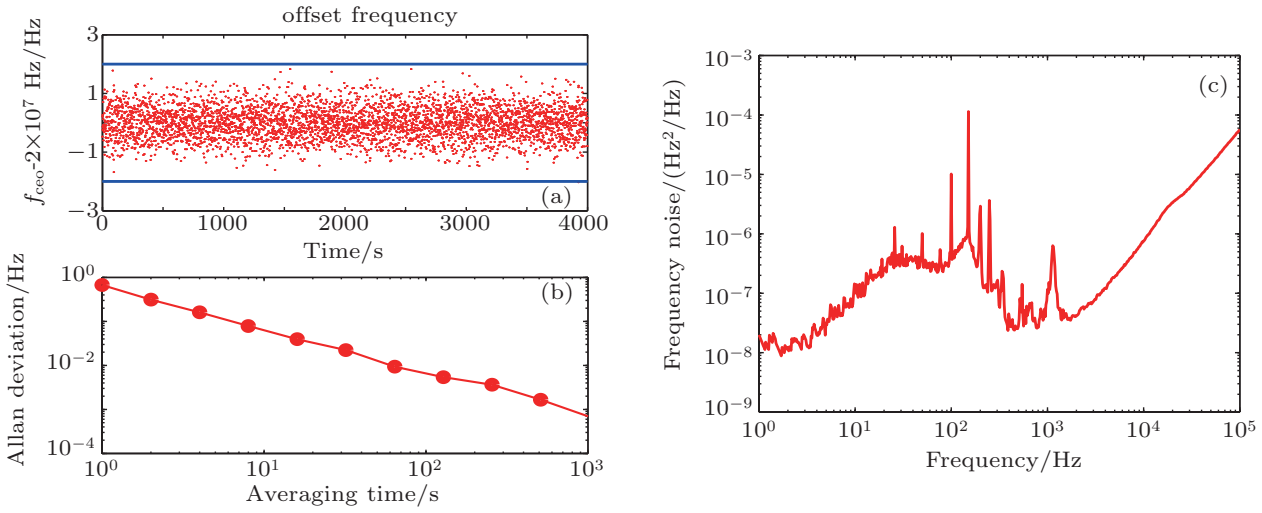


Fig. 3. (color online) Stabilities of locked f_{ceo} and f_{rep}. (a) Locked f_{ceo} with a gate time of 1 s. (b) The Allan deviation of locked f_{ceo} as a function of average time. (c) The frequency noise of locked f_{rep} derived from the power spectral density of phase noise.

The stabilities of f_{ceo} and f_{rep} are evaluated first. Achieved by a sequence of amplification, nonlinear spectrum boardening and second harmonic generation, the linewidth of f_{ceo} is on the order of several hundred kHz. It is better to evaluate this parameter via Allan deviation. We use a Π-type frequency counter with no dead time at a gate time of 1 s to record locked f_{ceo} for 4000 s. The result is shown in Fig. 3(a). A glitch exceeding the threshold is kicked out when calculating the Allan deviation. From Fig. 3(b), 1-s average time Allan deviation of locked f_{ceo} is ~ 0.66 Hz. The Allan deviation comes down as the average time increases. The power spectral density of the phase noise is suitable to locked f_{rep}. Figure 3(c) shows the frequency noise of locked f_{rep} with Fourier frequency from 1 Hz to 100 kHz. The integrated RMS residual frequency modulation df_{rep} is 1.4 Hz.

To obtain the interferometric signal, laser combs are

locked at different repetition rates, $f_{\mathrm{rep},1} = 250.000$ MHz and $f_{\mathrm{rep},2} = 250.002$ MHz. Thus, the difference Δf_{rep} is 2 kHz, and interferograms are repeatedly generated with a time interval of 0.5 ms. 25 interferograms are recorded within 12.5 ms. Figure 4(a) shows one of the interferograms. The dynamic range is optimized to 825. Free-induction decay (FID)[6] can be seen on both sides of the centerburst as both laser beams interact with the gas sample. According to the above parameters, we simulate dual-comb interferometric signals. Figure 4(b) shows one of 25 simulated interferograms. The FID signal is also clear around the centerburst. The simulation only takes laser frequency fluctuation into consideration.

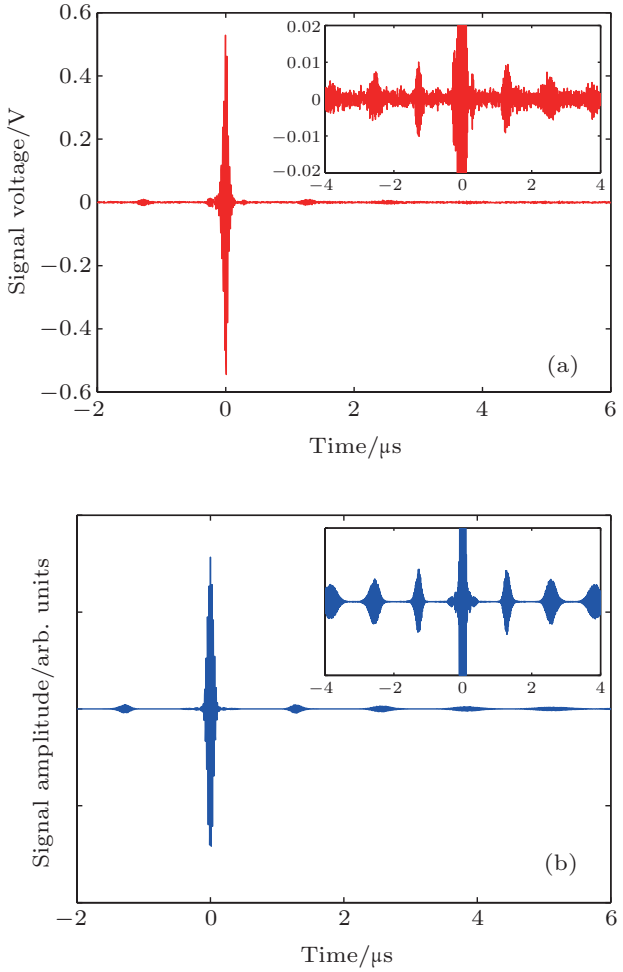


Fig. 4. (color online) (a) Interferometric signal of asynchronous dual laser combs. Inset: partial magnified free-induction decay (FID) signal. (b) Simulated interferometric signal.

Figure 5(a) shows six measured spectra. The sidelobes around the absorption peaks are suppressed due to apodization with a 12-μs triangular window. In order to average in the next step, all the interferograms are phase corrected. As laser frequency fluctuates during measurement, the absorption peak presents frequency jitter relative to the reference peak in the database, and the amplitude of the absorption peak also varies randomly.

The nominal conversion factor β is 1.25×10^5. As indicated in the previous analysis, a small fluctuation in f_{rep} leads to a considerable change in β, which further causes significant misalignment in up-conversion to the optical domain. With the parameters of the experimental setup, the RF comb is located around 46 MHz. Therefore, the RMS spectral frequency jitter is estimated from

$$|\Delta_{\mathrm{jitter}}| = |f_{\mathrm{RF}} \cdot \mathrm{d}\beta| = |f_{\mathrm{RF}} \cdot f_{\mathrm{rep}}/(\Delta f_{\mathrm{rep}})^2 \cdot \sqrt{2} \cdot \mathrm{d}f_{\mathrm{rep}}|$$

to be 0.19 cm^{-1}. Along the horizontal axis in Fig. 6, the frequency jitter of the measured absorption peak near 6446.16 cm^{-1} is within about ±0.3 cm^{-1} due to laser fluctuation during measurement. The standard deviation of the distribution is 0.20 cm^{-1}. Meanwhile, the frequency misalignment range in the simulation is slightly smaller than that in the measurement result, and the standard deviation of the simulation is 0.15 cm^{-1}. The relative intensity noise of the laser combs contributing to the amplitude-to-frequency noise probably results in the difference.[14] Further, we can simulate spectrum degradation according to laser performance. Along the vertical axis of Fig. 6, it can also be seen that the relative amplitude of the absorption peak changes due to not well-stabilized lasers. It can be speculated that that amplitude fluctuation will become more and more significant as the stability of the laser deteriorates.

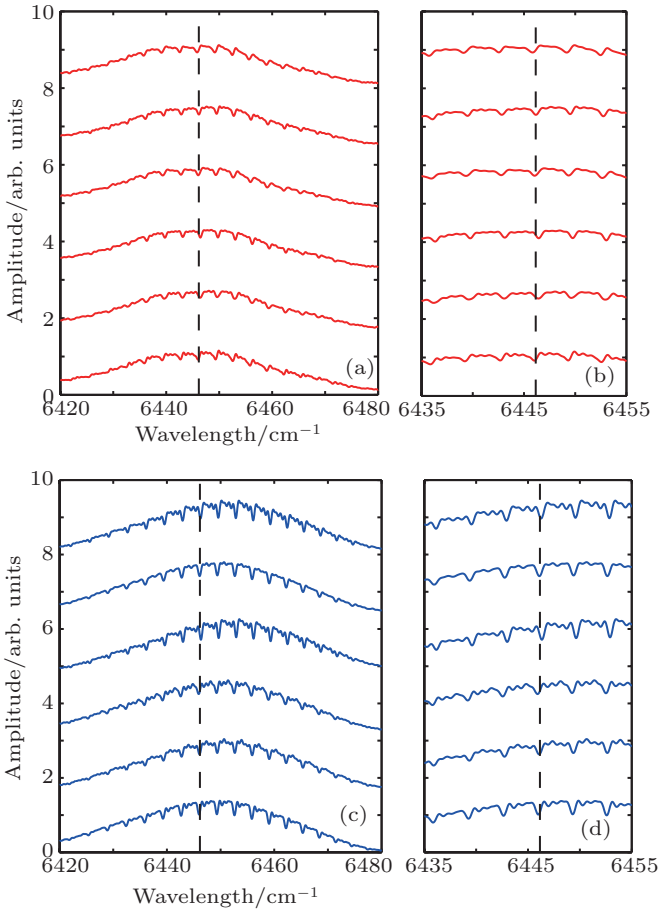


Fig. 5. (color online) Six spectra obtained from measurement (a) and simulation (c) are offset for viewing clarity. Panels (b) and (d) show the partially expanded curves in panels (a) and (c), respectively. The dashed line denotes the absorption peak at 6446.16 cm^{-1} from GEISA database.

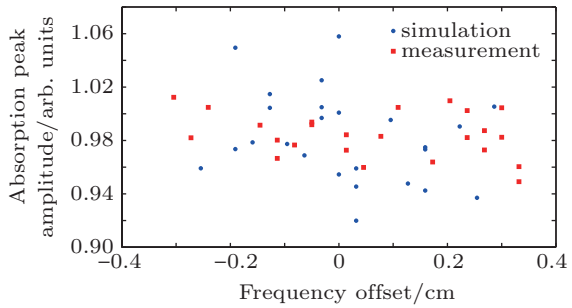


Fig. 6. (color online) Amplitude and frequency offset distributions of the absorption peak near 6446.16 cm^{-1} in the measured and simulated results.

Focusing on a narrow region of interest, the frequency jitter of each absorption peak in one spectrum could be approximately treated as a constant. Therefore, the measured spectra are dynamically modified one by one with respect to the absorption peak at 6446.16 cm^{-1}. In Fig. 7, we can compare the averaged spectra with and without frequency modification, and the simulated spectrum based on the GEISA database. The signal-to-noise ratio degrades by directly averaging unmodified spectra, while it is effectively improved in the averaged spectrum with modification. The spectral resolution is 0.8 cm^{-1}.

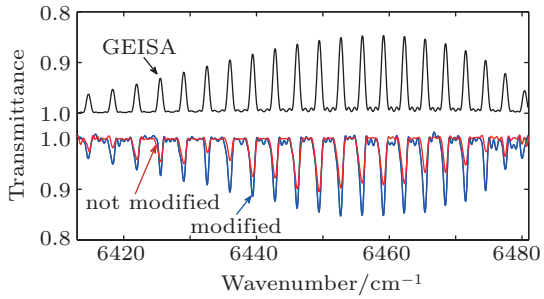


Fig. 7. (color online) Comparison between the averaged spetrum with and without modification and the simulation based on GEISA.

4. Discussion and conclusions

In this study, we demonstrate that the repetition rate fluctuation has a significant effect on spectral frequency misalignment by considering the inevitable phenomenon of laser fluctuation. By measuring the frequency noise of the repetition rate, the RMS residual frequency modulation of locked f_{rep} is 1.4 Hz in our system. According to the experimental setup, we simulate absorption peak jitter which is proven experimentally. By modifying the spectra with respect to the reference peak and averaging in the frequency domain, the signal-to-noise ratio is effectively improved. The averaged spectrum agrees well with the simulation result. However, this kind of modification is limited to the case of a low-resolution spectrometer. When it comes to high-resolution, more attention should be paid to the phase noises of both laser combs.

Further, the relative linewidth between laser combs is the most important parameter that seriously restricts the application of interferometric spectrometry. Next, a narrow linewidth cw laser is expected. By utilizing a phase-lock loop with a large control bandwidth, the phase noise of the comb mode that is offset-locked to the cw laser could be suppressed.[15,16] It will benefit the coherent averaging in the time domain.

References

[1] Udem T, Holzwarth R and Hansch T W 2002 *Nature* **416** 233
[2] Newbury N R 2011 *Nat. Photon.* **5** 186
[3] Griffiths P R, Haseth J A 2007 *Fourier Transform Infrared Spectrometry* (Hoboken: Wiley)
[4] Schiller S 2002 *Opt. Lett.* **27** 766
[5] Keilmann F, Gohle C and Holzwarth R 2004 *Opt. Lett.* **29** 1542
[6] Coddington I, Swann W C and Newbury N R 2010 *Opt. Lett.* **35** 1395
[7] Schliesser A, Brehm M, Keilmann F and Weide D 2005 *Opt. Express* **13** 9029
[8] Coddington I, Swann W C, Newbury N R 2008 *Phys. Rev. Lett.* **100** 013902
[9] Zolot A M, Giorgetta F R, Baumann E, Swann W C, Coddington I and Newbury N R 2013 *J. Quantum Spectrosc. Radiat. Transfer* **118** 26
[10] Ideguchi T, Poisson A, Guelachvili G, Picqué N and Hänsch T W 2014 *Nat. Commun.* **5** 3375
[11] Deschênes J D, Giaccari P and Genest J 2010 *Opt. Express* **18** 23358
[12] Roy J, Deschênes J D, Potvin S and Genest J 2012 *Opt. Express* **20** 21932
[13] Jones D J, Diddams S A, Ranka J K, Stenz A, Windler R S, Hall J L and Cundiff S T 2000 *Science* **288** 635
[14] Newbury N R, Coddington I, Swann W C 2010 *Opt. Express* **18** 7929
[15] Bartels A, Oates C W, Hollberg L and Diddams S A 2004 *Opt. Lett.* **29** 1081
[16] Benko C, Ruehl A, Martin M J, Eikema K S E, Fermann M E, Hartl I and Ye J 2012 *Opt. Lett.* **37** 2196